

Quantum control landscape for ultrafast generation of single-qubit phase shift quantum gates‡

Boris O Volkov¹, Oleg V Morzhin¹ and Alexander N Pechen^{1,2}

¹ Department of Mathematical Methods for Quantum Technologies, Steklov Mathematical Institute of Russian Academy of Sciences, 8 Gubkina Str., Moscow, 119991, Russia; www.mi-ras.ru/eng/dep51

² National University of Science and Technology "MISIS", 4 Leninsky Prosp., Moscow 119991, Russia

E-mail: borisvolkov1986@gmail.com, morzhin.oleg@yandex.ru,

Corresponding author: apechen@gmail.com; www.mathnet.ru/eng/person17991

Abstract. In this work, we consider the problem of ultrafast controlled generation of single-qubit phase shift quantum gates. Globally optimal control is a control which realizes the gate with maximal possible fidelity. Trap is a control which is optimal only locally but not globally. It was shown before that traps do not exist for controlled generation of arbitrary single-qubit quantum gates for sufficiently long times, as well as for fast control of quantum gates other than phase shift gates. Ultrafast generation of phase-shift gates was missed in the previous analysis. In this work we show, combining analytical and numerical optimization methods such as Gradient Ascent Pulse Engineering (GRAPE), differential evolution, and dual annealing, that control landscape for ultrafast generation of phase shift gates is also free of traps. Mathematical analysis of quantum control landscapes, which aims to prove either absence or existence of traps for quantum control objective functionals, is an important topic in quantum control. In this work, we provide a rigorous analysis of quantum control landscapes for ultrafast generation of single-qubit quantum gates and show, combining analytical methods based on a sophisticated analysis of spectrum of the Hessian, and numerical optimization methods such as Gradient Ascent Pulse Engineering (GRAPE), differential evolution, and dual annealing, that control landscape for ultrafast generation of phase shift gates is free of traps.

Keywords: quantum control, control landscape, qubit, phase shift gate

1. Introduction

Control of atomic and molecular systems is an important branch of modern science with various existing and prospective applications in various directions of quantum technologies [1, 2, 3, 4, 5, 6, 7, 8, 9]. In application to quantum computing, it can be used to generate with high fidelity quantum gates in a minimal time [10].

‡ Accepted for publication in *Journal of Physics A: Mathematical and Theoretical* on April 1, 2021. This Accepted Manuscript is available for reuse under a CC BY-NC-ND licence after the 12 month embargo period provided that all the terms of the licence are adhered to.

In this work we consider the problem of generating single qubit phase shift quantum gates. Single qubit phase shift gate with phase $\phi \in [0, 2\pi)$ in the computational basis can be represented as a unitary 2×2 matrix

$$R_\phi = \begin{pmatrix} 1 & 0 \\ 0 & e^{i\phi} \end{pmatrix}.$$

Up to an unphysical phase factor one has $R_\phi = W_{\phi/2}$, where $W_\phi = e^{i\phi\sigma_z}$ and σ_z is the z -Pauli matrix. On ultrafast time scale, the influence of the environment often can be negligible and the dynamics of the qubit can be approximately described by Schrödinger equation:

$$i\frac{dU_t^f}{dt} = (H_0 + f(t)V)U_t^f, \quad U_{t=0}^f = \mathbb{I}. \quad (1)$$

Here H_0 and V are the free and interaction Hamiltonians (Hermitian 2×2 -matrices), and f is a coherent control. The free and interaction Hamiltonians are assumed to be non-commutative, $[H_0, V] \neq 0$, to exclude trivial case.

Typical choices for the space of controls are the spaces $L^1 = L^1([0, T], \mathbb{R})$ and $L^2 = L^2([0, T], \mathbb{R})$ which consist of all Lebesgue measurable functions $f : [0, T] \rightarrow \mathbb{R}$ such that, correspondingly, $\int_0^T |f(t)| dt < \infty$ and $\int_0^T f^2(t) dt < \infty$ (strictly speaking, elements of these spaces are equivalence classes of functions which coincide almost everywhere). The latter is a subspace of the former, $L^2 \subset L^1$. The space L^1 is the most general space of controls for which the Schrödinger equation (1) by Carathéodory's existence theorem for every control f has a unique absolutely continuous solution. The space L^2 is a Hilbert space (while L^1 is not), and this property is convenient for Hessian analysis performed in this work. For this reason, we use L^2 in this work as the control space. For numerical optimization we use finite dimensional subspaces of piecewise constant controls defined explicitly in Sec. 5.2.

The goal of quantum control is to find a control f such that the induced evolution U_T^f is as close as possible to the target gate $W \in SU(2)$. The problem of generating a single qubit gate W can be formulated as problem of maximizing the objective functional,

$$J_W[f] = \frac{1}{4} |\text{Tr}(W^\dagger U_T^f)|^2 \rightarrow \max. \quad (2)$$

Indeed, the maximum value $J_W[f_*] = 1$ is attained if and only if the control f_* is such that $U_T^{f_*} = e^{i\alpha}W$ for some (physically irrelevant) phase α .

Trap is a control which is optimal only locally but not globally. The analysis of traps is important for practical design of control fields, where it can help to select between global and local search optimal control protocols. Global search protocols (e.g., genetic algorithms, simulated annealing, stochastic optimization) are the better choice if traps do exist, while local search protocols (e.g., gradient-type) are preferable if it is theoretically known that a given quantum control objective has no traps. In this situation local search protocols could be more efficient for finding optimal controls, while in the presence of traps their work can be hindered at a local maximum thereby

preventing arrival of the maximum of the objective functional. Choosing an efficient strategy is especially important for laboratory optimization, where high number of iterations of the protocol is a time/energy/cost expensive.

An important problem in quantum control is to investigate whether traps can or can not exist in quantum control landscapes [11, 12, 13, 14, 15, 16, 17, 18, 19, 20]. The problem in its completeness is not yet solved [21, 22]. Much effort is directed towards ultrafast control at quantum speed limit [23, 17, 24, 25, 26, 27, 28, 29, 30, 31]. For this case, the absence of traps for control landscape of a two-level Landau-Zener system at times around or greater quantum speed limit was rigorously proved in [17], and for some cases below quantum speed limit in [28, 32] (see also [33]). Numerical investigation of the control landscape for this system for a different from the present work control objective (transition probability) for times around the quantum speed limit was performed in [20]. Severe restrictions, e.g. considering piecewise constant controls with a small number of constant components, may destroy the trap-free property as shown for example on figure 1 in Ref. [17]. Thus when we discuss the absence of traps, we mean the restriction-free case with controls belonging to the functional space.

In this work we show, combining analytical and numerical results, that ultrafast generation of phase shift gates is also free of traps. The structure of the work is the following. In Sec. 2 we outline known results. In Sec. 3 main theoretical result of this work is formulated. Sec. 4 contains formulations and proofs of several lemmas which when combined give proof of the main theorem. Sec. 5 contains numerical analysis of the control landscape for various values of the parameters ϕ and T using Gradient Ascent Pulse Engineering (GRAPE) [34] stochastic zeroth-order optimization methods of differential evolution [35, 36] (DE) and dual annealing [37, 38, 39] (DA).

2. Previous results

In [17, 18] it was proved that if T is large enough then the control objective $J_W[f]$ for a qubit has no traps. Later in [32] for arbitrarily small time and for any W such that $W \neq e^{i\varphi_W \sigma_z}$ (i.e., for any target gate except of phase shift gates) it was proved that traps also do not exist. For phase-shift gates traps were shown to not exist for any $T > 0$ if $\varphi_W \in (0, \pi/2)$ and for any $T > \pi - \varphi_W$ if $\varphi_W \in [\frac{\pi}{2}, \pi]$, in the units when the Hamiltonian is properly normalized. The only absent up to now case has been the analysis of traps for generating phase-shift gates with $\varphi_W \in [\frac{\pi}{2}, \pi]$ at a small time.

To explicitly formulate these previously known results on the absence of traps for controlled single qubit gate generation, consider the special constant control $f(t) = f_0$ and time T_0 :

$$f_0 := \frac{-\text{Tr } H_0 \text{Tr } V + 2 \text{Tr}(H_0 V)}{(\text{Tr } V^2)^2 - 2 \text{Tr}(V^2)}, \quad (3)$$

$$T_0 := \frac{\pi}{\|H_0 - \mathbb{I} \text{Tr } H_0/2 + f_0(V - \mathbb{I} \text{Tr } V/2)\|}. \quad (4)$$

The following result was proved in [18, 32].

Theorem 1 *Let $W \in SU(2)$ be a single qubit quantum gate. If $[W, H_0 + f_0V] \neq 0$ then for any $T > 0$ traps do not exist. If $[W, H_0 + f_0V] = 0$ then any control, except possibly $f \equiv f_0$, is not trap for any $T > 0$ and the control f_0 is not trap for $T > T_0$.*

The case of whether control f_0 can be trap for $T \leq T_0$ was partially studied in [32]. Without loss of generality it is sufficient to consider the case $H_0 = \sigma_z$ and $V = v_x\sigma_x + v_y\sigma_y$, where $v_x, v_y \in \mathbb{R}$ ($v_x^2 + v_y^2 > 0$) and $\sigma_x, \sigma_y, \sigma_z$ are the Pauli matrices:

$$\sigma_x = \begin{pmatrix} 0 & 1 \\ 1 & 0 \end{pmatrix}, \quad \sigma_y = \begin{pmatrix} 0 & -i \\ i & 0 \end{pmatrix}, \quad \sigma_z = \begin{pmatrix} 1 & 0 \\ 0 & -1 \end{pmatrix}. \quad (5)$$

In this case, the special time is $T_0 = \frac{\pi}{2}$ and the special control is $f_0 = 0$.

By theorem 1, if $[W, \sigma_z] \neq 0$, then for any $T > 0$ there are no traps for J_W . If $[W, \sigma_z] = 0$, then $W = e^{i\varphi_W\sigma_z + i\beta}$, where $\varphi_W \in (0, \pi)$ and $\beta \in [0, 2\pi)$. The phase can be neglected, so without loss of generality we set $\beta = 0$. Below we consider only such gates. The following result was proved in [32].

Theorem 2 *Let $W = e^{i\varphi_W\sigma_z}$. If $\varphi_W \in (0, \frac{\pi}{2})$, then for any $T > 0$ there are no traps. If $\varphi_W \in [\frac{\pi}{2}, \pi]$, then for any $T > \pi - \varphi_W$ there are no traps.*

For fixed φ_W and T the value of the objective evaluated at f_0 is

$$J_W[f_0] = \cos^2(\varphi_W + T). \quad (6)$$

If $\varphi_W + T = \pi$ then $J_W[f_0] = 1$ and f_0 is a global maximum.

If $\varphi_W + T = \frac{\pi}{2}$ and $\varphi_W + T = \frac{3\pi}{2}$ then $J_W[f_0] = 0$ and f_0 is a global minimum.

In the present work we study the remaining case when $\varphi_W \in [\frac{\pi}{2}, \pi]$ and $T < \pi - \varphi_W$. In this case $J_W[f_0] < 1$. We prove that for this case the special control $f_0 = 0$ is a critical point for the objective functional J_W and that this point is not a saddle point. We prove that the Hessian of J_W at f_0 is an injective compact operator which has only negative eigenvalues. In this case f_0 could be either a (1) global maximum, (2) trap, or (3) trap in a more weak sense, such that a restriction of J_W to any finite dimensional subspace of $L^2([0, T], \mathbb{R})$ would have local maximum at f_0 while f_0 is not a point of global maximum. Performed numerical simulations show that the first case has place, i.e., f_0 is a point of global maximum, while giving a rigorous proof of this finding remains an open problem. The numerical results also show that for $\frac{\pi}{2} \leq \varphi_W \leq \pi$ and $0 < T \leq \frac{\pi}{2}$ achieving the objective functional value 1, i.e., providing exact generation of phase shift gate, requires minimal time $T_{\min} = \pi - \varphi_W$.

3. Main theorem

We use the notations $Y = W^\dagger U_T^f$ and $V_t = U_t^{f\dagger} V U_t^f$ as considered in Ref. [32].

The Taylor expansion of the functional J_W at f up to the second order has the form:

$$J_W[f + \delta f] = J_W[f] + \int_0^T \frac{\delta J_W}{\delta f(t)} \delta f(t) dt + \frac{1}{2} \int_0^T \int_0^T \text{Hess}(t, s) \delta f(t) \delta f(s) dt ds + o(\|\delta f\|_{L^2}^2), \quad \delta f \rightarrow 0. \quad (7)$$

The linear term is determined by the integral kernel of the Fréchet derivative,

$$\frac{\delta J_W}{\delta f(t)} = \frac{1}{2} \Im(\text{Tr} Y^* \text{Tr}(YV_t))$$

and determines the gradient of the objective; the second order term is the integral kernel of the Hessian,

$$\text{Hess}(t, s) = \begin{cases} \frac{1}{2} \Re(\text{Tr}(YV_t) \text{Tr}(Y^*V_s) - \text{Tr}(YV_sV_t) \text{Tr} Y^*), & \text{if } s \geq t \\ \frac{1}{2} \Re(\text{Tr}(YV_s) \text{Tr}(Y^*V_t) - \text{Tr}(YV_tV_s) \text{Tr} Y^*), & \text{if } s < t. \end{cases}$$

The control $f_0 = 0$ is a critical point, i.e., gradient of the objective evaluated at this control is zero. The Hessian at $f_0 = 0$ has the form (see [32]):

$$\text{Hess}(s, t) = -2v^2 \cos \varphi \cos(2|t - s| + \varphi), \quad (8)$$

where $\varphi = -\varphi_W - T$ and $v = \sqrt{v_x^2 + v_y^2}$.

Let us consider the following cases:

- (φ_W, T) belongs to the triangle domain

$$\mathcal{D}_1 := \left\{ (\varphi_W, T) : 0 < T < \frac{\pi}{2}, \quad \frac{\pi}{2} \leq \varphi_W < \pi - T \right\};$$

- (φ_W, T) belongs to the set

$$\mathcal{D}_2 := \left\{ (\varphi_W, T) : 0 < T \leq \frac{\pi}{2}, \quad \varphi_W = \pi - T \right\};$$

- (φ_W, T) belongs to the triangle domain

$$\mathcal{D}_3 := \left\{ (\varphi_W, T) : 0 < T \leq \frac{\pi}{2}, \quad \pi - T < \varphi_W \leq \pi, \quad (\varphi_W, T) \neq \left(\pi, \frac{\pi}{2}\right) \right\}.$$

- (φ_W, T) belongs to the square domain without the diagonal

$$\mathcal{D}_4 := \left\{ (\varphi_W, T) : 0 < T \leq \frac{\pi}{2}, \quad 0 < \varphi_W < \frac{\pi}{2}, \varphi_W + T \neq \frac{\pi}{2} \right\}.$$

Our main result is the following theorem.

Theorem 3 *If $(\varphi_W, T) \in \mathcal{D}_1 \cup \mathcal{D}_3 \cup \mathcal{D}_4$ then the Hessian of the objective functional J_W at $f_0 = 0$ is an injective compact operator on $L^2([0, T], \mathbb{R})$. Moreover,*

(i) *If $(\varphi_W, T) \in \mathcal{D}_1$, then Hessian at f_0 has only negative eigenvalues.*

(ii) *If $(\varphi_W, T) \in \mathcal{D}_3 \cup \mathcal{D}_4$ then Hessian at f_0 has both negative and positive eigenvalues.*

In this case, the special control $f_0 = 0$ is a saddle point for the objective functional.

Remark 1 *The second case was previously proved by Pechen and Il'in in [32] using a different method. The first case has not been previously considered and is a new result of this work.*

Remark 2 *As is mentioned in the introduction, in the previous works [18, 32] the case when the control belongs to the space $L^1([0, T], \mathbb{R})$ was considered. In this case the Schrödinger equation (1) by Carathéodory's existence theorem for every control f has a unique absolutely continuous solution.*

Let $\{e_n\}$ be an orthonormal basis in the Hilbert space $L^2([0, T], \mathbb{R})$, which consists of the eigenvectors of the operator Hess and $\{\lambda_n\}$ be the corresponding eigenvalues. Any $\delta f \in L^2([0, T], \mathbb{R})$ can be expanded in the Fourier series $\delta f = \sum_{i=1}^{\infty} c_i e_i$. Then for the quadratic form generated by Hess we have the expression

$$(\text{Hess } \delta f, \delta f) = \int_0^T \int_0^T \text{Hess}(t, s) \delta f(t) \delta f(s) dt ds = \sum_{i=1}^{\infty} \lambda_i c_i^2.$$

If all eigenvalues $\{\lambda_n\}$ are negative, then the quadratic form is strictly negative, i.e. $(\text{Hess } \delta f, \delta f) < 0$ for any $\delta f \neq 0$. In this case, f_0 is at least a strict local maximum on any finite dimensional subspace of $L^2([0, T], \mathbb{R})$. In difference to [18, 32], where controls $f \in L^1([0, T], \mathbb{R})$ were considered, in the present paper we consider the case $f \in L^2([0, T], \mathbb{R})$, because in general the vectors $\{e_n\}$ do not form the Schauder basis in the space $L^1([0, T], \mathbb{R})$.

Remark 3 A class of n -level systems with $n \geq 4$ which have traps was discovered in [19]. These traps are constant controls. The Hessian of the objective functional computed at these controls has the form

$$\text{Hess}(t, s) = A \cos(\varepsilon|t - s|) + B \sin(\varepsilon|t - s|) + C. \quad (9)$$

It was shown in [19] that if A , B , and C satisfy certain relations then the Hessian (9) is strictly sign-definite. For the Hessian (8) these relations do not hold and we can not use the method of [19] for analyzing this case. For this reason in the present paper we investigate the spectrum and eigenvalues of Hessian (8) to access properties of the control landscape.

4. Proof of the main theorem

In this section we will prove Theorem 3. First we will prove that if $(\varphi_W, T) \in \mathcal{D}_1 \cup \mathcal{D}_3 \cup \mathcal{D}_4$ then the Hessian of the objective functional J_W at $f_0 = 0$ is an injective compact operator on $L^2([0, T], \mathbb{R})$.

If $(\varphi_W, T) \in \mathcal{D}_1 \cup \mathcal{D}_3 \cup \mathcal{D}_4$, then $\sin 2\varphi = -\sin 2(\varphi_W + T) \neq 0$. Instead of Hessian, we can consider the integral operator $K = \frac{1}{v^2 \sin 2\varphi} \text{Hess}$ with integral kernel:

$$K(s, t) = -\frac{\cos(2|t - s| + \varphi)}{\sin \varphi}, \quad (10)$$

Let

$$\begin{aligned} h(t) = (Kg)(t) &= -\frac{1}{\sin \varphi} \int_0^T \cos(2|t - s| + \varphi) g(s) ds \\ &= -\frac{1}{\sin \varphi} \int_0^t \cos(2t - 2s + \varphi) g(s) ds \\ &\quad - \frac{1}{\sin \varphi} \int_t^T \cos(2s - 2t + \varphi) g(s) ds. \end{aligned}$$

Assume that the function g is continuous. Then $h = Kg$ is C^2 -smooth function on $[0, T]$. The first and second derivatives of h have the form

$$h'(t) = \frac{2}{\sin \varphi} \left(\int_0^t \sin(2t - 2s + \varphi)g(s)ds - \int_t^T \sin(2s - 2t + \varphi)g(s)ds \right), \quad (11)$$

$$h''(t) = \frac{4}{\sin \varphi} \left(\int_0^t \cos(2t - 2s + \varphi)g(s)ds + \int_t^T \cos(2s - 2t + \varphi)g(s)ds \right) + 4g(t) = -4h(t) + 4g(t). \quad (12)$$

So if g is continuous and $h = Kg$, then the following equality holds

$$h''(t) + 4h(t) = 4g(t). \quad (13)$$

Let us show that the equality (13) holds in the weak sense for an arbitrary $g \in L^2([0, T], \mathbb{R})$ and $h = Kg$. Consider an arbitrary test function f , i.e. $f \in C^\infty([0, T], \mathbb{R})$ and the support of f belongs to the open interval $(0, T)$. Fubini's theorem implies that

$$\langle f'', h \rangle = \int_0^T f''(t)(Kg)(t)dt = -\frac{1}{\sin \varphi} \int_0^T \left(\int_0^T f''(t) \cos(2|t - s| + \varphi)dt \right) g(s)ds. \quad (14)$$

The internal integral can be integrated two times by parts:

$$\int_0^T f''(t) \cos(2|t - s| + \varphi)dt = -4 \int_0^T f(t) \cos(2|t - s| + \varphi)dt - 4 \sin \varphi f(s). \quad (15)$$

Substituting this expression into (14), we obtain

$$\begin{aligned} \langle f, h'' \rangle &= \langle f'', h \rangle = \frac{4}{\sin \varphi} \int_0^T \left(\int_0^T f(t) \cos(2|t - s| + \varphi)dt + 4 \sin \varphi f(s) \right) g(s)ds \\ &= -4 \langle f, h \rangle + 4 \langle f, g \rangle. \end{aligned} \quad (16)$$

Thus equality (13) holds in the weak sense. As a result, we get that if $h = 0$, then $g = 0$. Hence the operator K is an injective compact operator on $L^2([0, T], \mathbb{R})$.

For any continuous g , we can find $h = Kg$ as a unique solution of ODE (13), which satisfies the initial conditions

$$h(0) = -\frac{1}{\sin \varphi} \int_0^T \cos(2s + \varphi)g(s)ds, \quad (17)$$

$$h'(0) = -\frac{2}{\sin \varphi} \int_0^T \sin(2s + \varphi)g(s)ds. \quad (18)$$

Let μ be an eigenvalue of the operator K and g be the corresponding eigenfunction, so that $h = Kg = \mu g$. Let $\lambda = 1/\mu$. Then using (13), we obtain that

$$h''(t) = 4(\lambda - 1)h(t). \quad (19)$$

In the following sections, we examine whether eigenvalue μ can be positive.

4.1. Case $\lambda < 1$

Consider the case $\lambda < 1$. Let $a^2 = 4(1 - \lambda)$ and $a > 0$. If h satisfies (19) then h has the form $h(t) = b \cos at + c \sin at$ and

$$g(t) = \frac{4 - a^2}{4}(b \cos at + c \sin at).$$

Substituting h and g in the initial condition (17), we obtain

$$\begin{aligned} h(0) = b &= -\frac{1}{\sin \varphi} \int_0^T \cos(2s + \varphi)g(s)ds \\ &= \frac{a^2 - 4}{4 \sin \varphi} b \int_0^T \cos(2t + \varphi) \cos at dt + \frac{a^2 - 4}{4 \sin \varphi} c \int_0^T \cos(2t + \varphi) \sin at dt. \end{aligned} \quad (20)$$

This equality can be rewritten in the form

$$0 = A_{11}(a)b + A_{12}(a)c, \quad (21)$$

where

$$\begin{aligned} A_{11}(a) &= 2 \sin \varphi - a \sin(aT) \cos(2T + \varphi) + 2 \cos(aT) \sin(2T + \varphi), \\ A_{12}(a) &= a \cos(aT) \cos(2T + \varphi) + 2 \sin(aT) \sin(2T + \varphi) - a \cos \varphi. \end{aligned}$$

Substituting h and g in the initial conditions (18), we obtain

$$\begin{aligned} h'(0) = ac &= -\frac{2}{\sin \varphi} \int_0^T \sin(2s + \varphi)g(s)ds \\ &= \frac{a^2 - 4}{2 \sin \varphi} b \int_0^T \sin(2t + \varphi) \cos(at) dt + \frac{a^2 - 4}{4 \sin \varphi} c \int_0^T \sin(2t + \varphi) \sin(at) dt. \end{aligned} \quad (22)$$

This equality can be rewritten in the form

$$0 = A_{21}(a)b + A_{22}(a)c, \quad (23)$$

where

$$\begin{aligned} A_{21}(a) &= a \sin(aT) \sin(2T + \varphi) + 2 \cos(aT) \cos(2T + \varphi) - 2 \cos \varphi, \\ A_{22}(a) &= -a \sin \varphi + 2 \sin(aT) \cos(2T + \varphi) - a \cos(aT) \sin(2T + \varphi). \end{aligned}$$

The function $g(t) = \frac{4-a^2}{4}(b \cos at + c \sin at)$ is an eigenfunction of the operator K with the eigenvalue $\mu = 1/\lambda = 4/(4 - a^2)$ if and only if $(x_1, x_2) = (b, c)$ is a nonzero solution of the linear system of equations

$$\begin{cases} A_{11}(a)x_1 + A_{12}(a)x_2 = 0 \\ A_{21}(a)x_1 + A_{22}(a)x_2 = 0. \end{cases} \quad (24)$$

Define the function of argument $a \in \mathbb{R}$

$$F_{\varphi_W, T}^1(a) = A_{11}(a)A_{22}(a) - A_{12}(a)A_{21}(a).$$

By direct computations we get

$$F_{\varphi_W, T}^1(a) = -4a - a^2 \sin(aT) \sin(2\varphi_W) - 4 \sin(aT) \sin(2\varphi_W) + 4a \cos(aT) \cos(2\varphi_W).$$

Nonzero solutions of the system (24) exists if and only if $F_{\varphi_W, T}^1(a) = 0$. Let us analyze positive roots of the function $F_{\varphi_W, T}^1$.

Lemma 1 *The function $F_{\varphi_W, T}^1$ has infinitely many roots in the interval $(2, +\infty)$ for any $(\varphi_W, T) \in \mathcal{D}_1 \cup \mathcal{D}_3 \cup \mathcal{D}_4$. Hence, operator K has infinitely many negative eigenvalues.*

Proof. If $\varphi_W \neq \frac{\pi}{2}$ and $\varphi_W \neq \pi$, then let $a_n = (-\frac{\pi}{2} + 2\pi n)/T$ and $a'_n = (\frac{\pi}{2} + 2\pi n)/T$. We have

$$F_{\varphi_W, T}^1(a_n) \sim \frac{(2\pi)^2}{T^2} \sin(2\varphi_W)n^2, \quad n \rightarrow +\infty,$$

$$F_{\varphi_W, T}^2(a'_n) \sim -\frac{(2\pi)^2}{T^2} \sin(2\varphi_W)n^2, \quad n \rightarrow +\infty.$$

The values of $F_{\varphi_W, T}^1(a_n)$ and $F_{\varphi_W, T}^1(a'_n)$ for sufficiently large n have different signs. Since to $F_{\varphi_W, T}^1$ is continuous, for sufficiently large n there exists at least one root of this function in the interval (a_n, a'_n) and at least one root in the interval (a'_n, a_{n+1}) .

If $\varphi_W = \frac{\pi}{2}$, then $a_n = \frac{\pi+2\pi n}{T}$ are roots of the function $F_{\varphi_W, T}^1$. If $\varphi_W = \pi$, then $a_n = \frac{2\pi n}{T}$ are roots of the function $F_{\varphi_W, T}^1$. This completes the proof.

Lemma 2 *If $(\varphi_W, T) \in \mathcal{D}_3$ such that $\varphi_W < \pi$, then $F_{\varphi_W, T}^1$ has a root in the interval $(0, 2)$. Hence in this case the operator K has at least one positive eigenvalue.*

Proof. The function $F_{\varphi_W, T}^1$ can be rewritten as

$$F_{\varphi_W, T}^1(a) = -4a - (a - 2)^2 \sin(aT) \sin(2\varphi_W) + 4a \cos(2\varphi_W + aT).$$

Let $a' = (2\pi - 2\varphi_W)/T$. If $(\varphi_W, T) \in \mathcal{D}_3$ such that $\varphi_W < \pi$, then we have $a' \in (0, 2)$. The following inequality holds

$$F_{\varphi_W, T}^1(a') = (a' - 2)^2 \sin^2(2\varphi_W) > 0.$$

If $(\varphi_W, T) \in \mathcal{D}_3$, then $\varphi \in (-\frac{3}{2}\pi, -\pi)$. Hence,

$$F_{\varphi_W, T}^1(2) = -16 \sin^2 \varphi < 0.$$

Since the function $F_{\varphi_W, T}^1$ is continuous, there exists a root of this function in the interval $(a', 2)$. This completes the proof.

Lemma 3 *If $(\varphi_W, T) \in \mathcal{D}_1$, then the function $F_{\varphi_W, T}^1$ has not roots in the interval $(0, 2)$.*

Proof. Fix any $a \in (0, 2)$. Let consider the function of two arguments $G_1(\varphi_W, T) = F_{\varphi_W, T}^1(a)$. In other words

$$G_1(\varphi_W, T) = -4a - (a^2 + 4) \sin(aT) \sin(2\varphi_W) + 4a \cos(aT) \cos(2\varphi_W).$$

Let consider the set $\text{int } \mathcal{D}_1$ of internal points of \mathcal{D}_1 , i.e.

$$\text{int } \mathcal{D}_1 = \{(\varphi_W, T): \varphi_W \in (\pi/2, \pi), T > 0, \varphi_W + T < \pi\}.$$

Let $\overline{\mathcal{D}_1}$ and $\partial\mathcal{D}_1$ denote the closure and the boundary of the set \mathcal{D}_1 . We have $\partial\mathcal{D}_1 = I_1 \cup I_2 \cup \mathcal{D}_2$, where $I_1 = \{(\pi/2, T): T \in [0, \pi/2]\}$, $I_2 = \{(\varphi_W, 0): \varphi_W \in [\pi/2, \pi]\}$.

Now we will prove that maximum value of G_1 is zero on the boundary $\partial\mathcal{D}_1$. Consider the cases:

(i) If $(\varphi_W, T) \in I_1$ then

$$G_1(\varphi_W, T) = G\left(\frac{\pi}{2}, T\right) = -4a - 4a \cos(aT) < 0.$$

(ii) If $(\varphi_W, T) \in I_2$ then

$$G_1(\varphi_W, T) = G_1(\varphi_W, 0) = -4a + 4a \cos(2\varphi_W) \leq 0.$$

Note that we have equality only if $(\varphi_W, T) = (\pi, 0)$.

(iii) Now let us show that $G_1(\varphi_W, T) < 0$ for all $(\varphi_W, T) \in \mathcal{D}_2$. For this purpose we consider the function $H_1(x) = G_1(\pi - x, x)$ for $x \in [0, \frac{1}{2}\pi]$,

$$H_1(x) = -4a + (a^2 + 4) \sin(ax) \sin(2x) + 4a \cos(ax) \cos(2x).$$

The derivative of H_1 is

$$H_1'(x) = \frac{1}{x}(a^2 - 4) \sin(2x) \sin(ax)(ax \cot(ax) - 2x \cot(2x)).$$

The function $f(x) = x \cot x$ strictly decreases in the interval $(0, \pi)$ and, hence, $ax \cot(ax) - 2x \cot(2x) > 0$ and $H_1'(x) < 0$ for all $x \in (0, \frac{\pi}{2})$. Thus the function H_1 strictly decreases in the closed interval $[0, \frac{\pi}{2}]$. Since $H_1(0) = 0$, we have $H_1(x) < 0$ for all $x \in (0, \frac{\pi}{2}]$. It implies that $G_1(\varphi_W, T) < 0$ for any $(\varphi_W, T) \in \mathcal{D}_2$.

Now we will show that the function G_1 has not critical points on $\text{int}\mathcal{D}_1$. Assume that there exists a critical point $(\varphi_W^*, T^*) \in \text{int}\mathcal{D}_1$. Then

$$\begin{cases} \partial_{\varphi_W} G_1(\varphi_W^*, T^*) = -2(a^2 + 4) \sin(aT^*) \cos(2\varphi_W^*) - 8a \cos(aT^*) \sin(2\varphi_W^*) = 0 \\ \partial_T G_1(\varphi_W^*, T^*) = -(a^2 + 4)a \cos(aT^*) \sin(2\varphi_W^*) - 4a^2 \sin(aT^*) \cos(2\varphi_W^*) = 0. \end{cases} \quad (25)$$

Due to $(\varphi_W^*, T^*) \in \text{int}\mathcal{D}_1$, we have $\sin(2\varphi_W^*) < 0$ and $\sin(aT^*) > 0$. Hence, system (25) can be rewritten as

$$\begin{cases} \frac{(a^2+4)}{4a} \cot(2\varphi_W^*) + \cot(aT^*) = 0 \\ \frac{4a}{(a^2+4)} \cot(2\varphi_W^*) + \cot(aT^*) = 0. \end{cases} \quad (26)$$

Due to $a \in (0, 2)$, we have $\frac{4a}{(a^2+4)} \neq \frac{(a^2+4)}{4a}$ and, hence, $\cot(2\varphi_W^*) = 0$ and $\cot(aT^*) = 0$. Then $\varphi_W^* = \frac{3\pi}{4}$. Due to $(\varphi_W^*, T^*) \in \text{int}\mathcal{D}_1$, we have that

$$0 < T^* < \pi - \varphi_W^* = \frac{\pi}{4}. \quad (27)$$

Hence, $aT^* \in (0, \frac{\pi}{2})$ and $\cot(aT^*) > 0$. We get a contradiction. The function G_1 has not critical points on the open set $\text{int}\mathcal{D}_1$. Hence, the function G_1 reaches its maximum value on $\overline{\mathcal{D}_1}$ at the boundary point $(\pi, 0)$. Due to the point $(\pi, 0)$ does not belong to \mathcal{D}_1 , we have

$$G_1(\varphi_W, T) < G_1(\pi, 0) = 0 \quad (28)$$

for all $(\varphi_W, T) \in \mathcal{D}_1$. Then $a \in (0, 2)$ is not a root of the function $F_{\varphi_W, T}^1$. This completes the proof.

4.2. Case $\lambda = 1$

If $\mu = 1$ is an eigenvalue of the operator K then the corresponding eigenfunctions should have the form

$$h(t) = g(t) = ct + b.$$

Substituting this function in the initial conditions (17), we obtain

$$h(0) = b = -\frac{1}{\sin \varphi} \int_0^T \cos(2t + \varphi)g(t)dt = -\frac{1}{\sin \varphi} \int_0^T \cos(2t + \varphi)(ct + b)dt. \quad (29)$$

This equality can be rewritten as

$$0 = B_{11}c + B_{12}b, \quad (30)$$

where

$$B_{11} = -\cos \varphi + \cos(\varphi + 2T) + 2T \sin(\varphi + 2T), \quad (31)$$

$$B_{12} = 2(\sin(2T + \varphi) + \sin \varphi). \quad (32)$$

Substituting h and g in the initial conditions (18), we obtain

$$h'(0) = c = -\frac{2}{\sin \varphi} \int_0^T \sin(2t + \varphi)g(t)dt = -\frac{2}{\sin \varphi} \int_0^T \sin(2t + \varphi)(ct + b)dt. \quad (33)$$

This equality can be rewritten as

$$0 = B_{21}c + B_{22}b, \quad (34)$$

where

$$B_{21} = \sin \varphi + \sin(\varphi + 2T) - 2T \cos(\varphi + 2T),$$

$$B_{22} = 2(-\cos(2T + \varphi) + \cos \varphi).$$

The function $g(t) = ct + b$ is an eigenfunction of the operator K with the eigenvalue $\mu = 1$ if and only if $(x_1, x_2) = (c, b)$ is a nonzero solution of the system of linear equations

$$\begin{cases} B_{11}x_1 + B_{12}x_2 = 0 \\ B_{21}x_1 + B_{22}x_2 = 0. \end{cases} \quad (35)$$

Such a solution exists if and only if

$$\Delta = B_{11}B_{22} - B_{12}B_{21} = -2 \sin \varphi_W (\sin \varphi_W + T \cos \varphi_W) = 0. \quad (36)$$

Lemma 4 *If $(\varphi_W, T) \in \mathcal{D}_1$ then $\mu = 1$ is not an eigenvalue of the operator K . If $(\varphi_W, T) \in \mathcal{D}_3$ such that $\varphi_W = \pi$ then $\mu = 1$ is an eigenvalue of the operator K .*

Proof. If $x \in (0, \frac{\pi}{2})$ then $0 < x < \tan x$. Hence, if $(\varphi_W, T) \in \mathcal{D}_1$, then

$$T < (\pi - \varphi_W) < \tan(\pi - \varphi_W) = -\tan \varphi_W.$$

Hence

$$\Delta = -2 \sin \varphi_W \cos \varphi_W (\tan \varphi_W + T) < 0.$$

and $\mu = 1$ does not belong to the spectrum of the operator K .

If $\varphi_W = \pi/2$ and $\varphi_W + T < \pi$, then

$$\Delta = -2 \sin \varphi_W (\sin \varphi_W + T \cos \varphi_W) = -2 \neq 0.$$

Hence, $\mu = 1$ is not an eigenvalue of K . The second statement of the lemma is trivial. This completes the proof.

4.3. Case $\lambda > 1$

Consider the case $\lambda > 1$. Let $a^2 = 4(\lambda - 1)$ and $a > 0$. If h satisfies (19) then h has the form $h(t) = be^{at} + ce^{-at}$. Then

$$g(t) = \frac{4 + a^2}{4}(be^{at} + ce^{-at}).$$

Substituting h and g in the initial condition (17) gives

$$\begin{aligned} h(0) &= (b + c) = -\frac{1}{\sin \varphi} \int_0^T \cos(2s + \varphi)g(s)ds \\ &= -\frac{a^2 + 4}{4 \sin \varphi} \left(b \int_0^T \cos(2t + \varphi)e^{at} dt + c \int_0^T \cos(2t + \varphi)e^{-at} dt \right). \end{aligned}$$

After calculating the integrals, this equality can be rewritten as

$$0 = C_{11}(a)b + C_{12}(a)c, \quad (37)$$

where

$$\begin{aligned} C_{11}(a) &= a \cos \varphi - 2 \sin \varphi - e^{aT} (a \cos(\varphi + 2T) + 2 \sin(\varphi + 2T)), \\ C_{12}(a) &= -a \cos \varphi - 2 \sin \varphi + e^{-aT} (a \cos(\varphi + 2T) - 2 \sin(\varphi + 2T)). \end{aligned}$$

Substituting h and g in the initial conditions (18) gives

$$\begin{aligned} h'(0) &= (ba - ca) = -\frac{2}{\sin \varphi} \int_0^T \sin(2s + \varphi)g(s)ds \\ &= -\frac{a^2 + 4}{2 \sin \varphi} \left(b \int_0^T \sin(2t + \varphi)e^{at} dt + c \int_0^T \sin(2t + \varphi)e^{-at} dt \right). \end{aligned}$$

After calculating the integrals, this equality can be rewritten as

$$0 = C_{21}(a)b + C_{22}(a)c, \quad (38)$$

where

$$\begin{aligned} C_{21}(a) &= a \sin \varphi + 2 \cos \varphi + e^{aT} (a \sin(\varphi + 2T) + 2 \cos(\varphi + 2T)), \\ C_{22}(a) &= -a \sin \varphi + 2 \cos \varphi - e^{-aT} (2 \cos(\varphi + 2T) + a \sin(\varphi + 2T)). \end{aligned}$$

The function $g(t) = \frac{4+a^2}{4}(be^{at} + ce^{-at})$ is an eigenfunction of the operator K with the eigenvalue $\mu = \frac{1}{\lambda} = \frac{4}{a^2+4}$ if and only if $(x_1, x_2) = (b, c)$ is a nonzero solution of the linear system

$$\begin{cases} C_{11}(a)x_1 + C_{12}(a)x_2 = 0 \\ C_{21}(a)x_1 + C_{22}(a)x_2 = 0. \end{cases} \quad (39)$$

Let us define the function of the argument a ,

$$F_{\varphi_W, T}^2(a) = C_{11}(a)C_{22}(a) - C_{12}(a)C_{21}(a).$$

Direct calculation gives the expression

$$\begin{aligned} F_{\varphi_W, T}^2(a) &= 8a - 2a^2 \sinh(aT) \sin(2\varphi_W) \\ &\quad - 8a \cosh(aT) \cos(2\varphi_W) + 8 \sinh(aT) \sin(2\varphi_W). \end{aligned} \quad (40)$$

Nonzero solutions of the system (39) exists if and only if $F_{\varphi_W, T}^2(a) = 0$.

Lemma 5 *If $(\varphi_W, T) \in \mathcal{D}_4$, then $F_{\varphi_W, T}^2$ has at least one positive root. Hence, in this case, the operator K has at least one positive eigenvalue.*

Proof. Consider the case $\varphi_W \in (0, \pi/2)$. Note that

$$\begin{aligned} F_{\varphi_W, T}^2(a) &\sim 8a(1 - \cos(2\varphi_W) + T \sin(2\varphi_W)), \quad a \rightarrow 0 + \\ F_{\varphi_W, T}^2(a) &\sim -a^2 e^{aT} \sin(2\varphi_W), \quad a \rightarrow +\infty. \end{aligned}$$

If $\varphi_W \in (0, \pi/2)$, then $\sin(2\varphi_W) > 0$ and hence,

$$(1 - \cos(2\varphi_W) + T \sin(2\varphi_W)) > 0.$$

For sufficiently small a one has $F_{\varphi_W, T}^2(a) > 0$, while for sufficiently large a one has $F_{\varphi_W, T}^2(a) < 0$. Since the function $F_{\varphi_W, T}^2$ is continuous, it has at least one positive root. This completes the proof.

Lemma 6 *If $(\varphi_W, T) \in \mathcal{D}_1$, then the function $F_{\varphi_W, T}^2$ has no positive roots.*

Proof. Fix any $a \in (0, 2)$. Consider the function of two arguments $G_2(\varphi_W, T) = F_{\varphi_W, T}^2(a)$,

$$G_2(\varphi_W, T) = 8a + 2(4 - a^2) \sinh(aT) \sin(2\varphi_W) - 8a \cosh(aT) \cos(2\varphi_W).$$

We show that the minimal value of G_2 is zero on the set $\partial\mathcal{D}_1$ separately for various cases:

(i) If $(\varphi_W, T) \in I_1$, then

$$G_2(\varphi_W, T) = G_2\left(\frac{\pi}{2}, T\right) = 8a + 8a \cosh(aT) > 0.$$

(ii) If $(\varphi_W, T) \in I_2$, then

$$G_2(\varphi_W, T) = G_2(\varphi_W, 0) = 8a - 8a \cos(2\varphi_W) \leq 0.$$

Note that we have the equality only if $(\varphi_W, T) = (\pi, 0)$.

(iii) Now let us show that $G_2(\varphi_W, T) < 0$ for all $(\varphi_W, T) \in \mathcal{D}_2$. For this purpose consider the function $H_2(x) = G_2(\pi - x, x)$, where $x \in [0, \pi/2]$. In other words,

$$H_2(x) = 8a + (2a^2 - 8) \sinh(ax) \sin(2x) - 8a \cosh(ax) \cos(2x).$$

The derivative of H_2 is

$$H_2'(x) = \frac{2}{x}(4 + a^2) \sin(2x) \sinh(ax)(ax \coth(ax) - 2x \cot(2x)).$$

For any $x \in (0, \frac{\pi}{2})$ the following estimates hold

$$\begin{aligned} 2x \cot(2x) &< 1 \\ ax \coth(ax) &> 1. \end{aligned}$$

This implies that $ax \coth(ax) - 2x \cot(2x) > 0$ and $H_2'(x) > 0$ for $x \in (0, \frac{\pi}{2})$. So the function H_2 strictly increases on $[0, \frac{\pi}{2}]$. Since $H_2(0) = 0$, we have $H_2(x) > 0$ for any $x \in (0, \frac{\pi}{2}]$. It means that $G_2(\varphi_W, T) > 0$ for any $(\varphi_W, T) \in \mathcal{D}_2$.

Now we will show that the function G_2 has no critical points on $\text{int}\mathcal{D}_1$. Assume that there exists a critical point $(\varphi_W^*, T^*) \in \text{int}\mathcal{D}_1$. Then

$$\begin{cases} \partial_{\varphi_W} G_2(\varphi_W^*, T^*) = 4(4 - a^2) \sinh(aT^*) \cos(2\varphi_W^*) + 16a \cosh(aT^*) \sin(2\varphi_W^*) = 0 \\ \partial_T G_2(\varphi_W^*, T^*) = 2a(4 - a^2) \cosh(aT^*) \sin(2\varphi_W^*) - 8a^2 \sinh(aT^*) \cos(2\varphi_W^*) = 0. \end{cases} \quad (41)$$

If $(\varphi_W^*, T^*) \in \text{int}\mathcal{D}_1$, then $\sin(2\varphi_W^*) < 0$ and $\sinh(aT^*) > 0$. Hence, system (41) can be rewritten as

$$\begin{cases} \frac{4-a^2}{4a} \cot(2\varphi_W^*) + \coth(aT^*) = 0 \\ \frac{4a}{a^2-4} \cot(2\varphi_W^*) + \coth(aT^*) = 0. \end{cases} \quad (42)$$

Since $\frac{4-a^2}{4a} \neq \frac{4a}{a^2-4}$, we have $\cot(2\varphi_W^*) = 0$ and $\coth(aT^*) = 0$. But $\coth(aT^*) > 0$. We got a contradiction. The function G_2 has not critical points on the open set $\text{int}\mathcal{D}_1$. Hence, the function G_2 reaches its minimum value on $\overline{\mathcal{D}_1}$ at the boundary point $(\pi, 0)$. Due to the point $(\pi, 0)$ does not belong to \mathcal{D}_1 , we have

$$G_2(\varphi_W, T) > G_2(\pi, 0) = 0 \quad (43)$$

for all $(\varphi_W, T) \in \mathcal{D}_1$. Then $a \in (0, 2)$ is not a root of the function $F_{\varphi_W, T}^2$. This completes the proof.

4.4. Proof of the main theorem.

In the case $(\varphi_W, T) \in \mathcal{D}_1$, Lemmas 1, 3, 4, 6 together imply that K has only negative eigenvalues and, hence, Hess has only negative eigenvalues. If $(\varphi_W, T) \in \mathcal{D}_3$, Lemmas 1, 2, 4 together imply that K has both negative and positive eigenvalues. If $(\varphi_W, T) \in \mathcal{D}_4$, Lemmas 1, 5 together imply that K has both negative and positive eigenvalues. So, in the case $(\varphi_W, T) \in \mathcal{D}_3 \cup \mathcal{D}_4$, the operator Hess has both negative and positive eigenvalues and f_0 is a saddle point of the objective functional.

5. Numerical analysis showing when $f_0 = 0$ is a global maximum

5.1. Reduction to finite-dimensional optimization

The theoretical analysis above shows that Hessian computed at the control $f_0 = 0$ is negative definite. However, this analysis does not say whether control f_0 is a global maximum of the objective functional J_W , or it is a trap for J_W , or it is a trap in the weak sense such that if space of controls is restricted to class of piecewise controls $PConst([0, T], Q) \subset L^2([0, T], \mathbb{R})$, where Q is a compact set, then f_0 is a local but not global maximum of J_W . Below we compute the exact analytical form of the objective for piecewise constant controls, and numerically analyze the landscape using GRAPE [34] through fminunc function built in MATLAB and also DE, DA through their implementations available in the library SciPy.

Due to the invariance property for $J_W[f]$ with respect to θ (see Lemma 5 in [32]), it is sufficient to fix $\theta = 0$.

In the square domain

$$\mathcal{D} := \mathcal{D}_1 \cup \mathcal{D}_2 \cup \mathcal{D}_3 \cup \left(\pi, \frac{\pi}{2}\right) = \left\{(\varphi_W, T) : \frac{\pi}{2} \leq \varphi_W \leq \pi, \quad 0 < T \leq \frac{\pi}{2}\right\},$$

consider the uniform grid

$$\mathcal{G}(\mathcal{D}) := \left\{(\varphi_W^j, T_i) : \varphi_W^j = \frac{\pi}{2} + \frac{\pi}{20}j, \quad j = \overline{0, 10}, \quad T_i = \frac{\pi}{20}i, \quad i = \overline{1, 10}\right\}, \quad (44)$$

which consists of 110 nodes shown on figure 1. The grid $\mathcal{G}(\mathcal{D}_1)$ (correspondingly, $\mathcal{G}(\mathcal{D}_2)$ and $\mathcal{G}(\mathcal{D}_3 \cup (\pi, \frac{\pi}{2}))$) consists of the nodes of $\mathcal{G}(\mathcal{D})$ which belong to \mathcal{D}_1 (correspondingly, to \mathcal{D}_2 and to $\mathcal{D}_3 \cup (\pi, \frac{\pi}{2})$). The numerical results below show that in the domains \mathcal{D}_1 and \mathcal{D}_2 the control f_0 is a global maximum of the objective functional $J_W[f]$, in addition to the shown above analytically fact that $J_W[f_0] = 1$ for $(\varphi_W, T) \in \mathcal{D}_2$.

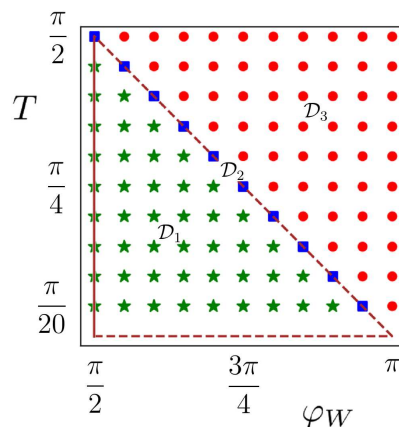


Figure 1. The grid $\mathcal{G}(\mathcal{D})$: 45 star green markers show the nodes in \mathcal{D}_1 , 10 square blue markers show the nodes in \mathcal{D}_2 , and 55 circle red markers show the nodes in $\mathcal{D}_3 \cup (\pi, \frac{\pi}{2})$. The triangle boundary of the set \mathcal{D}_1 is shown by dotted and solid lines; the points on both dotted lines do not belong to \mathcal{D}_1 .

5.2. Exact form of the objective function for piecewise constant controls

For each node (φ_W^j, T_i) , we restrict the space of controls to the set of piecewise constant controls

$$f(t) = \sum_{k=1}^K a_k \chi_{[t_k, t_{k+1})}(t), \quad (45)$$

where $a_k \in \mathbb{R}$ is the control amplitude during time interval $[t_k, t_{k+1})$ and $\chi_{[t_k, t_{k+1})}$ is the characteristic function of this time interval. Uniform spacing is considered so that $t_{k+1} = k\delta t$, where $\delta t = T_i/K$. For the final time T_i , we take $K = 2i$. The minimal value $K = 2$ corresponds to the case $T = T_1 = \pi/20$ (see on figure 1 the bottom horizontal line of the nodes); the maximal value $K = 20$ corresponds to the case $T = T_{10} = \pi/2$ (see the upper horizontal line of the nodes). The value $\delta t = \pi/40$ is the same for all i .

Control now is vector $\mathbf{a} = (a_1, \dots, a_K) \in \mathbb{R}^K$. For GRAPE, no restrictions on a_k are placed. For stochastic methods, the control amplitudes are bounded, so that for some $\nu > 0$:

$$-\nu < a_k < \nu, \quad k = 1, \dots, K.$$

For piecewise constant controls of the form (45), the evolution operator is the product of evolution operators at all time intervals,

$$U_T^{\mathbf{a}} = U_K \dots U_k \dots U_1,$$

where $U_k = e^{-i(\sigma_z + a_k \sigma_x) \delta t}$. Evolution operator U_k can easily be computed analytically using product rules for Pauli matrices. Indeed, for $A_k = -(\sigma_z + a_k \sigma_x) \delta t$ one has $A_k^2 = \delta t^2 (1 + a_k^2) \cdot \mathbb{I}_2$. Therefore

$$\begin{aligned} U_k = e^{iA_k} &= \sum_{n=0}^{\infty} \frac{(iA_k)^n}{n!} = \sum_{n=0}^{\infty} \frac{(iA_k)^{2n}}{2n!} + \sum_{n=0}^{\infty} \frac{(iA_k)^{2n+1}}{(2n+1)!} = \cos \alpha_k + iA_k \frac{\sin \alpha_k}{\alpha_k} \\ &= \cos \alpha_k - i\delta t (\sigma_z + a_k \sigma_x) \frac{\sin \alpha_k}{\alpha_k}, \end{aligned}$$

where $\alpha_k = \delta t \sqrt{1 + a_k^2}$. Thus, using sinc function $\text{sinc } \alpha = \sin \alpha / \alpha$, we get

$$U_T^{\mathbf{a}} = \left(\cos \alpha_K - i\delta t (\sigma_z + a_K \sigma_x) \text{sinc } \alpha_K \right) \dots \left(\cos \alpha_1 - i\delta t (\sigma_z + a_1 \sigma_x) \text{sinc } \alpha_1 \right). \quad (46)$$

This allows to write the objective as a function of the control,

$$J_W[\mathbf{a}] = \frac{1}{4} |\text{Tr}(W^\dagger U_T^{\mathbf{a}})|^2 \rightarrow \max_{\mathbf{a}} \quad (47)$$

(the maximum is taken over $\mathbf{a} \in \mathbb{R}^K$ for GRAPE and over $\mathbf{a} \in [-\nu, \nu]^K$ for DE and DA).

5.3. GRAPE optimization

GRAPE can be conveniently applied for quantum control problems in cases when gradient of the objective can be analytically computed. Its first advantage is the ability to use analytical expression for the gradient. Second advantage is that GRAPE does not require setting constraints on the amplitude of the control. Third advantage for our control problem is that in the functional space of controls any control other than f_0 was proved to be not trap (while restricting the space of controls to piecewise constant controls with fixed K can produce traps).

For this problem, we compute gradient of the objective

$$\text{grad} J_W[\mathbf{a}] = \frac{1}{2} \Im [\text{Tr}(Y^\dagger) \text{Tr}(Y V_k)].$$

Here

$$\begin{aligned} Y &= W^\dagger U_T^{\mathbf{a}}, \\ V_k &= U_k^\dagger \dots U_1^\dagger V U_1 \dots U_k. \end{aligned}$$

The algorithm starts by randomly generating, with the uniform distribution, the initial control $\mathbf{a}_0 = (a_1, \dots, a_n)$ where each $a_k \in [-A; A]$ ($A = 1$ is chosen), and then shifting

the control using the computed gradient value. For implementing GRAPE, we apply built in MATLAB function `fminunc` for unconstrained optimization using value and gradient of the objective ($-J_W[\mathbf{a}]$). In numerical simulations, for each node we make runs of GRAPE starting with two random initial points.

5.4. Differential evolution and dual annealing methods

The methods of DE and DA are zeroth-order optimization methods which use only values of the objective function and do not use gradient, Hessian, etc. These methods are stochastic methods used for an approximate global optimization. They were applied for example for numerical optimization of coherent and incoherent controls in an open quantum system [41, 42]. Since the SciPy library gives implementations of these methods to minimize the objective, the problem $-J_W[\mathbf{a}] \rightarrow \min_{\mathbf{a} \in [-\nu, \nu]^K}$ is considered. For numerical integration of the dynamical system, the tool `odeint` [40] available in the SciPy library is used. Taking into account the stochastic nature of DE and DA methods, we carry out two runs of each method for each node (φ_W^j, T_i) with a subsequent comparison of the results of all runs.

5.5. The numerical simulations for the grid $\mathcal{G}(\mathcal{D}_1)$

In the domain \mathcal{D}_1 , for each $l \in \text{Ind}(\mathcal{G}(\mathcal{D}_1))$: (1) we numerically find the optimized vector $\mathbf{a} = \hat{\mathbf{a}}^l$ and the corresponding maximal value \hat{J}_W^l of the objective function $J_W[\mathbf{a}]$ using GRAPE without constraints on the amplitude of the control, as well as the methods of DE and DA for $\nu = 50$; (2) compare the maximized value of the objective function with the value $J_W^l[0]$.

On the grid $\mathcal{G}(\mathcal{D}_1)$, the minimal value among the values $\{\hat{J}_W^l\}$ is close to 0.0245, and the maximal value is close 0.9755. In other words, exact generation of phase shift gate is not attained for any node of the grid $\mathcal{G}(\mathcal{D}_1)$. On figure 2 (a), 45 star green markers show the values of J_W on this grid. Figure 2 (b) shows the graph of the table-defined function

$$\{\Delta_l\} := \{\hat{J}_W^l - J_W^l[0]\} \quad (48)$$

corresponding to the grid $\mathcal{G}(\mathcal{D})$. For the grid $\mathcal{G}(\mathcal{D}_1)$, 45 star green markers at the bottom in figure 2 (b) illustrate optimality of the control f_0 . We have $\min_{l \in \text{Ind}(\mathcal{G}(\mathcal{D}_1))} \{|\Delta_l|\} \approx 4 \cdot 10^{-9}$, $\max_{l \in \text{Ind}(\mathcal{G}(\mathcal{D}_1))} \{|\Delta_l|\} \approx 2 \cdot 10^{-7}$, and $\frac{1}{45} \sum_{l \in \text{Ind}(\mathcal{G}(\mathcal{D}_1))} |\Delta_l| \approx 6 \cdot 10^{-8}$. Figure 2 (c) shows the cumulative distribution function for the values $\{\log_{10} |\Delta_l| : l \in \text{Ind}(\mathcal{G}(\mathcal{D}_1))\}$. The computed values of the function $\{\hat{J}_W^l\}_{l \in \text{Ind}(\mathcal{G}(\mathcal{D}_1))}$ are given in table 1. The computed values of the function $\{\Delta_l\}_{l \in \text{Ind}(\mathcal{G}(\mathcal{D}_1))}$ are given in table 2. Thus, we conclude that for each node of the grid $\mathcal{G}(\mathcal{D}_1)$ the value \hat{J}_W^l found by the optimization methods and the value $J_W^l[0]$ computed at the control f_0 coincide with high accuracy.

All 45 numerically optimized controls are represented by 330 values forming the

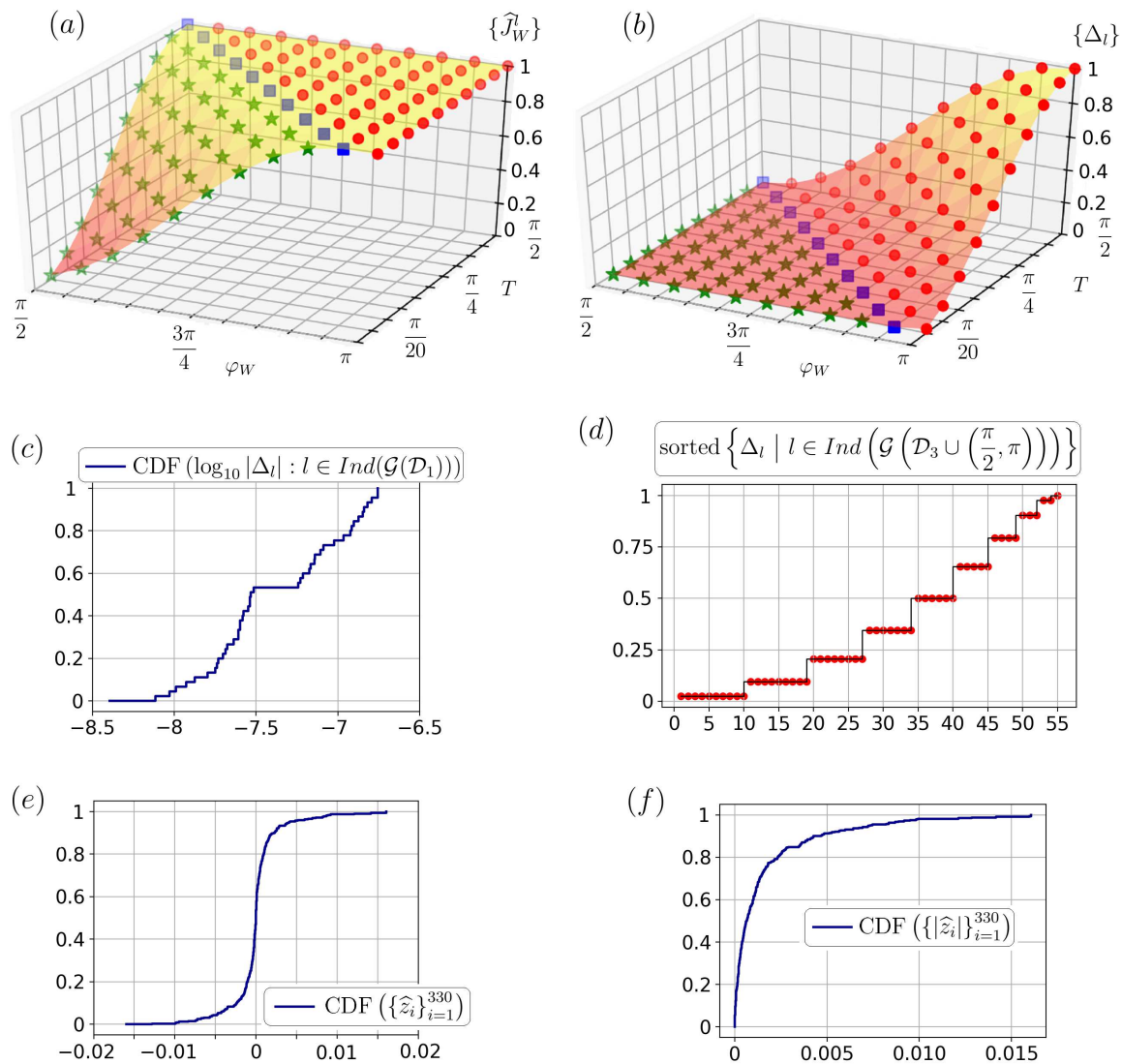


Figure 2. Subplots (a) and (b) show the table-defined functions $\{\widehat{J}_W\}$ and $\{\Delta_l\}$ obtained using GRAPE, the methods of DE and DA (for the last two methods $\nu = 50$ is taken); the corresponding interpolation surfaces are also shown. Here 45 star green markers show points corresponding to the grid $\mathcal{G}(\mathcal{D}_1)$; 10 square blue markers show points corresponding to the grid $\mathcal{G}(\mathcal{D}_2)$; 55 circle red markers show points corresponding to the grid $\mathcal{G}(\mathcal{D}_3 \cup (\frac{\pi}{2}, \pi))$. Other subplots illustrate the results computed using the methods of DE and DA. Subplot (c) shows the cumulative distribution function for $\{\log_{10} |\Delta_l| : l \in \text{Ind}(\mathcal{G}(\mathcal{D}_1))\}$. Subplot (d) shows 55 sorted values Δ_l for $l \in \text{Ind}(\mathcal{G}(\mathcal{D}_3 \cup (\frac{\pi}{2}, \pi)))$. With respect to the grid $\mathcal{G}(\mathcal{D}_1)$, subplots (e) and (f) show the cumulative distribution functions for $\{\widehat{z}_i\}_{i=1}^{330}$ and $\{|\widehat{z}_i|\}_{i=1}^{330}$, correspondingly.

array

$$\widehat{\mathbf{z}} = \{\widehat{z}_i\}_{i=1}^{330} := \{\widehat{\mathbf{a}}_k^l : k = \overline{1, K_l}, l \in \text{Ind}(\mathcal{G}(\mathcal{D}_1))\}.$$

We find that $\min_{1 \leq i \leq 330} \{z_i\} \approx -0.02$, $\max_{1 \leq i \leq 330} \{z_i\} \approx 0.02$, $\min_{1 \leq i \leq 330} \{|z_i|\} \approx 5 \cdot 10^{-7}$, and

$\frac{1}{330} \sum_{i=1}^{330} |z_i| \approx 0.002$. Figure 2 (e, f) show the cumulative distribution functions for the

arrays $\{z_i\}_{i=1}^{330}$ and $\{|z_i|\}_{i=1}^{330}$, correspondingly. About 90 % of the values $\{\widehat{z}_i\}_{i=1}^{330}$ are located between -0.005 and 0.005 . Thus, we conclude that the all 45 numerically optimized piecewise constant controls are close to the control f_0 .

5.6. The numerical simulations for the grid $\mathcal{G}(\mathcal{D}_2)$

According to (6) we have $J_W[0] = 1$ for any $(\varphi_W, T) \in \mathcal{D}_2$. Numerically we also find that with high accuracy $\widehat{J}_W^l \approx 1$ for any $l \in \text{Ind}(\mathcal{G}(\mathcal{D}_2))$. The values of the function $\{\widehat{J}_W^l\}_{l \in \text{Ind}(\mathcal{G}(\mathcal{D}_2))}$ are given in table 1. On figure 2 (b) 10 square blue markers show differences Δ_l for the grid $\mathcal{G}(\mathcal{D}_2)$. The mean value is $\frac{1}{10} \sum_{l \in \text{Ind}(\mathcal{G}(\mathcal{D}_2))} |\Delta_l| \approx 6 \cdot 10^{-6}$. All these ten differences almost equal to zero.

5.7. The numerical simulations for the grid $\mathcal{G}(\mathcal{D}_3 \cup (\pi, \frac{\pi}{2}))$

Using the numerical optimization methods, we find that for any node of the grid $\mathcal{G}(\mathcal{D}_3 \cup (\pi, \frac{\pi}{2}))$ the maximum value $\{\widehat{J}_W^l\}$ of the objective functional J_W is almost equal to 1. This is illustrated by 55 circle red markers in figure 2 (a). The values of Δ_l for the grid $\mathcal{G}(\mathcal{D}_3 \cup (\pi, \frac{\pi}{2}))$ are shown by 55 circle red markers on figure 2 (b). We obtain $\min_{l \in \text{Ind}(\mathcal{G}(\mathcal{D}_3 \cup (\pi, \frac{\pi}{2})))} \{|\Delta_l|\} \approx 0.0024$, $\max_{l \in \text{Ind}(\mathcal{G}(\mathcal{D}_3 \cup (\pi, \frac{\pi}{2})))} \{|\Delta_l|\} \approx 1$, and $\frac{1}{55} \sum_{l \in \text{Ind}(\mathcal{G}(\mathcal{D}_3 \cup (\pi, \frac{\pi}{2})))} |\Delta_l| \approx 0.37$. Figure 2 (d) shows sorted values of Δ_l . The values of $\{\widehat{J}_W^l\}_{l \in \text{Ind}(\mathcal{G}(\mathcal{D}_3 \cup (\pi, \frac{\pi}{2})))}$ are shown in table 1. The values of $\{\Delta_l\}_{l \in \text{Ind}(\mathcal{G}(\mathcal{D}_3 \cup (\pi, \frac{\pi}{2})))}$ are shown in table 2. For each node of $\mathcal{G}(\mathcal{D}_3 \cup (\pi, \frac{\pi}{2}))$, comparing the maximum value \widehat{J}_W^l obtained using the optimization methods with the value $J_W^l[0]$ informs that the control f_0 is not globally optimal for this grid.

All 55 numerically optimized piecewise constant controls are represented by 770 values forming the array

$$\widehat{\mathbf{z}} = \{\widehat{z}_i\}_{i=1}^{770} := \left\{ \widehat{\mathbf{a}}_k^l : k = \overline{1, K_l}, l \in \text{Ind} \left(\mathcal{G} \left(\mathcal{D}_3 \cup \left(\pi, \frac{\pi}{2} \right) \right) \right) \right\}.$$

This array is characterized by $\min_{1 \leq i \leq 770} \{z_i\} \approx -50$, $\max_{1 \leq i \leq 770} \{z_i\} \approx 50$, $\min_{1 \leq i \leq 770} \{|z_i|\} \approx 0.002$, and $\frac{1}{770} \sum_{i=1}^{770} |z_i| \approx 18$.

5.8. Minimal final times

As figure 2 (a) shows, if we fix the value φ_W^j and look for a minimal time to reach the boundary value $J_W = 1$, then we can take

$$T_i = \pi - \varphi_W^j, \quad j \in \overline{0, 10}, \quad i \in \overline{1, 10}, \quad f(t) = 0 \quad \forall t \in [0, T_i],$$

i.e. we can take the corresponding node of the grid $\mathcal{G}(\mathcal{D}_2)$ and the control f_0 .

Table 1. The obtained values (up to three digits) of the function $\{\widehat{J}_W^l\}_{l=1}^{110}$ for the grid (44). The values are shown on figure 2 (a).

$T_i \backslash \varphi_W^j$	φ_W^1	φ_W^2	φ_W^3	φ_W^4	φ_W^5	φ_W^6	φ_W^7	φ_W^8	φ_W^9	φ_W^{10}	φ_W^{11}
T_{10}	1.0	1.0	1.0	1.0	1.0	1.0	1.0	1.0	1.0	1.0	1.0
T_9	0.976	1.0	1.0	1.0	1.0	1.0	1.0	1.0	1.0	1.0	1.0
T_8	0.905	0.976	1.0	1.0	1.0	1.0	1.0	1.0	1.0	1.0	1.0
T_7	0.794	0.905	0.976	1.0	1.0	1.0	1.0	1.0	1.0	1.0	1.0
T_6	0.655	0.794	0.905	0.976	1.0	1.0	1.0	1.0	1.0	1.0	1.0
T_5	0.5	0.655	0.794	0.905	0.976	1.0	1.0	1.0	1.0	1.0	1.0
T_4	0.345	0.5	0.655	0.794	0.905	0.976	1.0	1.0	1.0	1.0	1.0
T_3	0.206	0.345	0.5	0.655	0.794	0.905	0.976	1.0	1.0	1.0	1.0
T_2	0.095	0.206	0.345	0.5	0.655	0.794	0.905	0.976	1.0	1.0	1.0
T_1	0.024	0.095	0.206	0.345	0.5	0.655	0.794	0.905	0.976	1.0	1.0

Table 2. The obtained values (up to three digits) of the function $\{\Delta_l\}_{l=1}^{110}$ for the grid (44). The values are shown on figure 2 (b).

$T_i \backslash \varphi_W^j$	φ_W^1	φ_W^2	φ_W^3	φ_W^4	φ_W^5	φ_W^6	φ_W^7	φ_W^8	φ_W^9	φ_W^{10}	φ_W^{11}
T_{10}	0	0.024	0.095	0.206	0.345	0.5	0.655	0.794	0.905	0.976	1.0
T_9	0	0	0.024	0.095	0.206	0.345	0.5	0.655	0.794	0.905	0.976
T_8	0	0	0	0.024	0.095	0.206	0.345	0.5	0.655	0.794	0.905
T_7	0	0	0	0	0.024	0.095	0.206	0.345	0.5	0.655	0.794
T_6	0	0	0	0	0	0.024	0.095	0.206	0.345	0.5	0.655
T_5	0	0	0	0	0	0	0.024	0.095	0.206	0.345	0.5
T_4	0	0	0	0	0	0	0	0.024	0.095	0.206	0.345
T_3	0	0	0	0	0	0	0	0	0.024	0.095	0.206
T_2	0	0	0	0	0	0	0	0	0	0.024	0.095
T_1	0	0	0	0	0	0	0	0	0	0	0.024

5.9. The piecewise constant controls with two variables

In this subsection we consider the case $K = 2$ and $T_1 = \pi/20$, so that $\delta T = T_1/K = T/2$. This case is considered as it allows for a simple visualization of the typical structure of the control landscape, similarly to that done in [17, 20] for a different objective functional. The objective functional $J_W[f]$ in this case reduces to the objective function $J_W[\mathbf{a}]$ of $\mathbf{a} = (a_1, a_2) \in \mathbb{R}^2$.

With the notations $\alpha_i = \delta t \sqrt{1 + a_i^2}$ for $i = 1, 2$, the objective function takes the exact analytical form

$$\begin{aligned}
J_W[\mathbf{a}] = & 2 \cos \phi_W \left\{ \cos \alpha_1 \cos \alpha_2 - \delta t^2 (1 + a_1 a_2) \operatorname{sinc} \alpha_1 \operatorname{sinc} \alpha_2 \right\} \\
& - 2 \delta t \sin \phi_W \left\{ \operatorname{sinc} \alpha_1 \cos \alpha_2 + \operatorname{sinc} \alpha_2 \cos \alpha_1 \right\}.
\end{aligned} \tag{49}$$

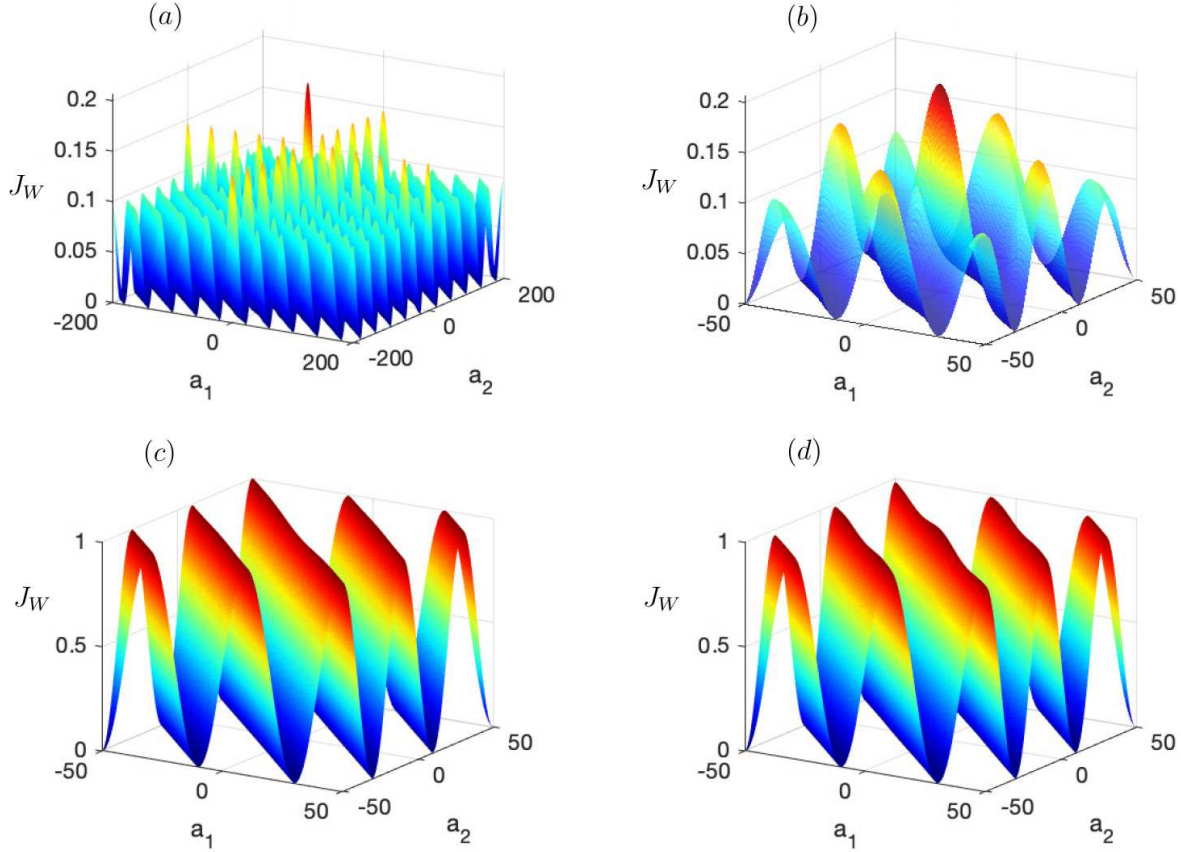


Figure 3. The dynamical control landscapes for $T_1 = \pi/20$ and $K = 2$: (a), (b) for $(\varphi_W, T_1) = (\frac{3\pi}{5}, \frac{\pi}{20}) \in \mathcal{G}(\mathcal{D}_1)$; (c) for $(\varphi_W, T_1) = (\pi, \frac{\pi}{20}) \in \mathcal{G}(\mathcal{D}_3)$; (d) for $(\varphi_W, T_1) = (\frac{19\pi}{20}, \frac{\pi}{20}) \in \mathcal{G}(\mathcal{D}_2)$.

Define on the set $[-\nu, \nu] \times [-\nu, \nu]$ the uniform grid with the step $\Delta a = 1$,

$$\left\{ (a_1^s, a_2^q) : a_1^s = -\nu + s\Delta a, \quad s = \overline{0, N}, \quad a_2^q = -\nu + q\Delta a; \quad q = \overline{0, N}, \quad \Delta a = \frac{2\nu}{N} \right\}.$$

For each node (a_1^s, a_2^q) , the corresponding control is denoted as $f^{s,q}$. Consider the cases $(\varphi_W, T_1) = (\frac{3\pi}{5}, \frac{\pi}{20}) \in \mathcal{G}(\mathcal{D}_1)$, $(\varphi_W, T_1) = (\frac{19\pi}{20}, \frac{\pi}{20}) \in \mathcal{G}(\mathcal{D}_2)$, and $(\varphi_W, T_1) = (\pi, \frac{\pi}{20}) \in \mathcal{G}(\mathcal{D}_3)$. For each case, the corresponding control landscape is plotted on figure 3 by computing the values of the objective function $J_W[\mathbf{a}]$ for each node (a_1^s, a_2^q) . The presence of traps in these control landscapes is due to the strong constraints posed by the form of the control. Subplots (a) and (b) for the node $(\varphi_W, T_1) = (\frac{3\pi}{5}, \frac{\pi}{20}) \in \mathcal{D}_1$ show that: (1) $\mathbf{a} = (0, 0)$ is a global maximum with the objective value significantly smaller than 1; (2) traps exist. Subplot (c) for the node $(\varphi_W, T_1) = (\pi, \frac{\pi}{20}) \in \mathcal{D}_3$, shows that $\mathbf{a} = (0, 0)$ is a saddle point. In this case, the maximum value $J_W[\mathbf{a}] = 1$ is reachable (in table 1, see for the case (φ_W^1, T_1)), but not at $\mathbf{a} = (0, 0)$. Subplot (d) for the node $(\varphi_W, T_1) = (\frac{19\pi}{20}, \frac{\pi}{20}) \in \mathcal{D}_2$ shows that the global maximum with objective value 1 is achieved at $\mathbf{a} = (0, 0)$ implying precise generation of the quantum gate by the control f_0 .

6. Conclusion

In this work, we studied the problem of ultrafast controlled generation of single-qubit phase shift quantum gates. This problem can be reduced to the problem of maximization of the objective functional J_W parameterized by $\varphi_W \in (0, \pi]$ in the case of the fixed time $T < T_0 = \pi/2$. In [32] it was proved that the only possible trap for this objective functional is the special control $f_0 = 0$ and it could potentially be trap only if $\varphi_W \in [\frac{\pi}{2}, \pi]$ and $T < \pi - \varphi_W$. It was known that this special control under these conditions is a critical point of the objective functional, but it was not known whether it is a saddle point, a global extremum point, or a trap. In this paper, we have investigated the Hessian of the objective functional J_W at f_0 for various values $\varphi_W \in (0, \pi]$ and for small times T . In this case, the Hessian is an integral self-adjoint operator. Considering the inverse differential operator to the Hessian, we investigated its spectrum and eigenvalues. We show that for $\varphi_W \in [\frac{\pi}{2}, \pi]$ and $T \in (\pi - \varphi_W, \frac{\pi}{2})$ and for $\varphi_W \in (0, \frac{\pi}{2})$ and $T \in (0, \frac{\pi}{2}]$ such that $\varphi_W + T \neq \frac{\pi}{2}$ the special control $f_0 = 0$ is a saddle point of the objective functional J_W . This result was previously obtained in [32] by another method. A new result of this paper is the proof that for $\varphi_W \in [\frac{\pi}{2}, \pi]$ and $T < \pi - \varphi_W$ the Hessian is a negative definite operator. Thus, it is rigorously proved that in this case f_0 is either a global maximum point, a trap, or a trap in the weak sense. The numerical analysis is further performed to show that this control is a global maximum point. The numerical results also show that for $\frac{\pi}{2} \leq \varphi_W \leq \pi$ and $0 < T \leq \frac{\pi}{2}$ achieving the objective functional value 1, i.e., providing exact generation of phase shift gate, requires a final time T being not less than the minimal time $T_{\min} = \pi - \varphi_W$. The exploited method based on Hessian analysis is potentially quite general and could be applied to the analysis of control landscapes for multi-level quantum systems and other control problems such as maximizing the transition probability to a target state and optimizing average value of a target observable, while the exact analysis may often be problem specific.

Acknowledgments

This work was funded by Russian Federation represented by the Ministry of Science and Higher Education (grant number 075-15-2020-788).

References

- [1] Shapiro M and Brumer P 2012 *Quantum Control of Molecular Processes. Second, Revised and Enlarged Edition* (Weinheim: WILEY-VCH Verlag GmbH & Co. KGaA)
- [2] Rice S A and Zhao M 2000 *Optical Control of Molecular Dynamics* (New York: John Wiley & Sons, Inc.)
- [3] Tannor D J 2007 *Introduction to Quantum Mechanics: A Time Dependent Perspective* (Sausalito: University Science Press)
- [4] Letokhov V S 2007 *Laser Control of Atoms and Molecules* (Oxford: Oxford Univ. Press)
- [5] D'Alessandro D 2008 *Introduction to Quantum Control and Dynamics* (Boca Raton: Chapman & Hall/CRC).

- [6] Moore K W, Pechen A, Feng X-J, Dominy J, Beltrani V J, Rabitz H 2011 *Physical Chemistry Chemical Physics* **13**:21 10048–10070
- [7] Brif C, Chakrabarti R and Rabitz H 2012 *Advances in Chemical Physics* ed. S A Rice and A R Dinner (Hoboken, New Jersey: John Wiley & Sons, Inc.) **148** 1–76
- [8] Khodjasteh K, Lidar D A and Viola L 2010 *Phys. Rev. Lett.* **104**:9 090501
- [9] Glaser S J, Boscain U, Calarco T, Koch C P, Köckenberger W, Kosloff R, Kuprov I, Luy B, Schirmer S, Schulte-Herbrüggen T, Sugny D and Wilhelm F K 2015 *Eur. Phys. J. D* **69**:12 279
- [10] Arute F, Arya K, Babbush R *et al* 2019 *Nature* **574**:7779 505–510
- [11] Rabitz H A, Hsieh M M and Rosenthal C M 2004 *Science* **303**:5666 1998–2001
- [12] Ho T-S and Rabitz H 2006 *J. Photochem. Photobiol. A: Chem.* **180**:3 226–240
- [13] Chakrabarti R and Rabitz H 2007 *Int. Rev. Phys. Chem.* **26**:4 671–735
- [14] Pechen A, Prokhorenko D, Wu R and Rabitz H 2008 *J. Phys. A: Math. Theor.* **41**:4 045205
- [15] Wu R, Pechen A, Rabitz H, Hsieh M and Tsou B 2008 *J. Math. Phys.* **49**:2 022108
- [16] Pechen A N and Tannor D J 2011 *Phys. Rev. Lett.* **106**:12 120402
- [17] Pechen A and Il'in N 2012 *Phys. Rev. A* **86**:5 052117
- [18] Pechen A N and Il'in N B 2014 *Proc. Steklov Inst. Math.* **285**:1 233–240
- [19] de Fouquieres P and Schirmer S G 2013 *Infin. Dimens. Anal. Quantum Probab. Relat. Top.* **16**:3 1350021
- [20] Larocca M, Poggi P M and Wisniacki D A 2018 *J. Phys. A: Math. Theor.* **51**:38 385305
- [21] Zhdanov D V 2018 *J. Phys. A: Math. Theor.* **51** 508001
- [22] Russell B, Wu R and Rabitz H 2018 *J. Phys. A: Math. Theor.* **51** 508002
- [23] Caneva T, Murphy M, Calarco T, Fazio R, Montangero S, Giovannetti V and Santoro G E 2009 *Phys. Rev. Lett.* **103**:24 240501
- [24] Bason M G, Viteau M, Malossi N, Huillery P, Arimondo E, Ciampini D, Fazio R, Giovannetti V, Mannella R and Morsch O 2012 *Nature Physics* **8** 147–152
- [25] Hegerfeldt G C 2013 *Phys. Rev. Lett.* **111**:26 260501
- [26] Avinadav C, Fischer R, London P and Gershoni D 2014 *Phys. Rev. B* **89**:24 245311
- [27] Hegerfeldt G C 2014 *Phys. Rev. A* **90**:3 032110
- [28] Pechen A and Il'in N 2017 *J. Phys. A: Math. Theor.* **50**:7 075301
- [29] Mortensen H L, Sørensen J J W H, Mølmer K and Sherson J F 2018 *New J. Phys.* **20** 025009
- [30] Lin C, Sels D and Wang Y 2020 *Phys. Rev. A* **101**:2 022320
- [31] Lam M R, Peter N, Groh T, Alt W, Robens C, Meschede D, Negretti A, Montangero S, Calarco T and Alberti A 2021 *Phys. Rev. X* **11**:1 011035
- [32] Il'in N B and Pechen A N 2016 *Izvestiya: Mathematics* **80**:6 1200–1212
- [33] Il'in N B and Pechen A N 2018 *Proc. Steklov Inst. Math.* **301**:1 109–113
- [34] Khaneja N, Reiss T., Kehlet C, Schulte-Herbrüggen T and Glaser S J 2005 *J. Magn. Reson.* **172**:2 296–305
- [35] Differential Evolution in SciPy: `scipy.optimize.differential_evolution`, https://docs.scipy.org/doc/scipy/reference/generated/scipy.optimize.differential_evolution.html
- [36] Storn R and Price K 1997 *J. Glob. Optim.* **11**, 341–359
- [37] Dual Annealing in SciPy: `scipy.optimize.dual_annealing`, https://docs.scipy.org/doc/scipy/reference/generated/scipy.optimize.dual_annealing.html
- [38] Tsallis C and Stariolo D A 1996 *Physica A* **233**:1–2 395–406
- [39] Xiang Y and Gong X G 2000 *Phys. Rev. E* **62**:3 4473–4476
- [40] Integrate a system of ordinary differential equations: `scipy.integrate.odeint`, <https://docs.scipy.org/doc/scipy/reference/generated/scipy.integrate.odeint.html>
- [41] Morzhin O V and Pechen A N 2020 *Phys. Part. Nuclei* **51**:4 464–469
- [42] Morzhin O V and Pechen A N 2020 *Lobachevskii J. Math.* **41**:12 2353–2368